PHYSICAL REVIEW A VOLUME 15, NUMBER 6 JUNE 1977

Low-energy electron-molecule scattering: Application of coupled-channel theory to e-CO_2 collisions*

Michael A. Morrison†
Department of Physics, Rice University, Houston, Texas 77001
and Theoretical Division (T-12), Los Alamos Scientific Laboratory, Los Alamos, New Mexico 87545

Neal F. Lane‡ and Lee A. Collins
Joint Institute for Laboratory Astrophysics, University of Colorado and National Bureau of Standards, Boulder, Colorado 80309
(Received 19 October 1976)

A theoretical coupled-channels investigation of e-CO_2 scattering is reported for incident electron energies from 0.07 to 10.0 eV. The fixed-nuclei approximation is made with the molecule in the ground $X\,^1\Sigma_g^+$ state and the nuclei frozen at their equilibrium positions. The e-CO_2 interaction potential consists of an *ab initio* electrostatic Hartree potential, an approximate local exchange potential, and a semiempirical polarization potential. The coupled-channel equations are formulated in a body-fixed reference frame using single-center coordinates and are solved by means of an integral-equations algorithm. Convergence of the highly anisotropic interaction potential and of the expansion of the scattering function are discussed. The asymptotic decoupling approximation and the Born approximation are also studied and found to be unsatisfactory methods for computing quantitatively accurate cross sections for low-energy e-CO_2 collisions. Converged coupled-channel total integrated, momentum-transfer and differential cross sections are presented, and the former are compared with experimental results, with special attention given to low scattering energies ($\lesssim$0.1 eV).

I. INTRODUCTION

In recent years, there has been considerable activity in the theoretical study of low-energy electron-molecule scattering.[1] With attention focused primarily on diatomic targets, progress has been made using three different approaches: (i) weak-scattering approximation methods (e.g., the Born approximation,[2] the distorted-waves method[3]), (ii) techniques based on eigenfunction expansions (e.g., close coupling[4-6]), and (iii) L^2-variational methods (e.g., R matrix,[7] T-matrix expansion,[8] pseudo-bound-state,[9] low-l spoiling[10]). Methods of the first type are frequently appropriate at very low energies for special cases (e.g., rotational excitation) where long-range multipole potentials dominate the scattering.[11] Eigenfunction expansion techniques have been applied with success to low-energy elastic electron scattering and to rotationally and vibrationally inelastic scattering from small diatomic targets. The final class of procedures are the newest and least tested, but results to date are highly promising. Very few applications of the latter two approaches to electron-polyatomic molecule collisions have been reported.[12]

One polyatomic target of considerable interest is carbon dioxide. Cross sections for electron scattering from CO_2 are relevant, for example, to studies of planetary atmospheres[13] and to the laser-fusion effort.[14] Considerable experimental research has been done on $e-CO_2$ collisions,[15-21] beginning with the crossed-beam measurements of elastic scattering of Ramsauer and Kollath[15] in 1930. Momentum-transfer cross sections have been determined by Phelps and collaborators[18-20] in swarm experiments, where anomalously large values are obtained at energies below ~0.1 eV. Similar behavior was seen in cyclotron resonance experiments by Tice and Kivelson,[17] who suggested that this phenomenon was due to scattering of the electron from a dipole potential caused by the instantaneous (transient) dipole moment seen during "zero-point" bending vibrations of the target.

At higher energies, a prominent resonance in the elastic and momentum-transfer cross sections is observed with a peak at 3.8 eV. First seen as fine structure in the elastic scattering cross section by Boness and Hasted,[22] this feature of the scattering has been extensively studied experimentally. Schulz and collaborators[23,24,21] have measured vibrational excitation cross sections for $e-CO_2$ scattering and observed structure in the vicinity of the resonance. In addition, Phelps *et al.* have determined cross sections for vibrational excitation.[19,20]

Comparatively little theoretical attention has been given to $e-CO_2$ collisions. Claydon *et al.*[25] used a semiempirical approximation to the SCF procedure to estimate the potential energy curves for several "resonance" CO_2^- states and thereby interpret various characteristics observed in such collision processes. These authors comment on the aforementioned 3.8-eV resonance, demonstrating that it reflects the formation of a $^2\Pi_u$ compound state with CO_2 in the linear nuclear con-

figuration. This resonance has also been discussed by Bardsley[26] and others.[27] Nonresonant vibrational excitation has been studied by Itikawa,[28] using the Born approximation and dipole matrix elements drawn from spectroscopic data.

Recently, we became interested in the empirical fact that low-energy momentum-transfer cross sections in CO_2 (Refs. 19 and 20) are observed to be considerably larger[18,29] than those of nonpolar diatomics (e.g., N_2) or even of some weakly *polar* molecules (e.g., N_2O). But CO_2 in its ground electronic and vibrational states is linear, on the average, and hence possesses no permanent dipole moment. It seems unlikely to us that the observed results are due to a transient dipole moment,[17,30] since at energies below the vibrational threshold, the "transient" dipole is felt only through *virtual* vibrational excitation. This is a second-order effect that can be represented by a polarization contribution to the potential energy, which varies at large r like r^{-4}. In electron-polar molecule scattering, it is the r^{-2} behavior of the permanent dipole interaction potential energy that gives rise to very large cross sections at low electron energies.

Therefore we undertook a study of $e - CO_2$ scattering using a coupled-channels procedure confining our attention to incident electron energies from 0.07 to 10.0 eV. Working in the fixed-nucleus approximation,[31] we have calculated total and momentum-transfer cross sections for a model electron—CO_2 interaction which includes an *ab initio* electrostatic interaction potential, an approximate local exchange potential, and a semiempirical polarization potential. The details of this theory are discussed in Sec. II. The coupled equations which obtain from this analysis are solved using the integral equations algorithm[32] together with certain modifications necessary to treat numerical problems resulting from the large number of partial waves required for convergence. This computational procedure is outlined in Sec. III. In Sec. IV, we present converged eigenphases and cross sections for $e - CO_2$ collisions and discuss briefly relevant convergence properties, sensitivity of the results to changes in our representation of the electron-molecule interaction potential, and asymptotic mixing of partial waves. Section V includes comments on limitations of this work and concludes the paper. Unless otherwise stated, atomic units are used throughout.

II. THEORY (REF. 33)

A. Scattering equations

We chose to formulate the collision problem in a single-center body-fixed coordinate system.[5] Thus the origin of coordinates is located at the center-of-mass of the molecule (for CO_2, the carbon nucleus), and the z axis is chosen to lie along the internuclear axis of the target, i.e., $\hat{z} = \hat{R}$. While prolate spheroidal coordinates have certain advantages in the study of electron collisions with diatomic targets,[34] the presence of the central carbon atom in CO_2 makes them less appropriate in this case, and we shall work in spherical polar coordinates.[35] The choice of a body-fixed coordinate system is consistent with the *fixed-nuclei approximation*,[31] which we shall employ. Thus we freeze the orientation in space of the target (specified by $\hat{R}$) throughout the collision, making the scattering function in the body-fixed frame independent of $\hat{R}$. One can calculate total and momentum-transfer cross sections by transforming to a laboratory-fixed reference frame and averaging over molecular orientations.[5] This approximation should be excellent for $e - CO_2$ collisions in the range of scattering energies under consideration, since[36] the energy spacing of the low-lying rotational levels in the ground electronic and vibrational state of the target is of the order 10^{-4} eV.

We further make the approximation that the internuclear separations are frozen at their equilibrium values, which for CO_2 corresponds to an oxygen-carbon separation of $R_{O\text{-}C} = 2.1944 a_0$. At very low energies, this is a reasonable assumption. However, the vibrational energy levels in CO_2 begin[26] at 0.17 eV (symmetric stretch), 0.08 eV (bending), and 0.29 eV (asymmetric stretch). We shall discuss the extent to which the neglect of these channels might affect our results in Sec. V.

Within this approximation, the nonrelativistic time-independent Schrödinger equation for scattering at energy $E = \frac{1}{2}k^2$ can be written

$$(\mathcal{H} - \tfrac{1}{2}k^2)\psi_k(\tau, \vec{r}) = 0, \tag{2.1}$$

where τ denotes the coordinates of the target electrons and $\vec{r}$ those of the scattered electron (we have suppressed the parametric dependence on R). The Hamiltonian is

$$\mathcal{H} = \mathcal{H}_{\text{target}} - \tfrac{1}{2}\nabla^2 + V_{\text{int}}(\tau, \vec{r}), \tag{2.2}$$

where $\mathcal{H}_{\text{target}}$ is the target molecular Hamiltonian and the ∇^2 operator is defined with respect to $\vec{r}$. In this equation V_{int} is the electrostatic interaction potential energy

$$V_{\text{int}} = -\sum_{\alpha} \frac{Z_\alpha}{|\vec{r} - \vec{R}_\alpha|} + \sum_i \frac{1}{|\vec{r} - \vec{r}_i|}, \tag{2.3}$$

with the first sum running over the nuclei of charge Z_α and the second over the bound molecular electrons.

The system wave function is expanded in elec-

tronic-state wave functions, eigenfunctions of $\mathcal{H}_{\text{target}}$, and then only the ground state ($^1\Sigma_g^+$) retained, leading to an equation for the scattering function, which we denote $F_k(\vec{r})$, viz.,

$$[\nabla^2 - 2V(\vec{r}) + k^2]F_k(\vec{r}) = 0, \tag{2.4}$$

where $V(\vec{r})$ is the electrostatic interaction potential $V_{\text{int}}(\tau, \vec{r})$ averaged over the ground electronic state. Note that we *do not antisymmetrize* in the coordinate of the scattering electron; doing so would lead to the presence in Eq. (2.4) of an additional term containing the exchange kernel.[37] Instead, we shall add an approximate local exchange potential (to be described in Sec. II B) to the static term. Finally, the truncation of the electronic-states expansion to a single term is a rather severe approximation even at very low energies, and neglects the important long-range polarization interaction as well as various short-range correlation contributions. We can partially account for the former by adding to $V(\vec{r})$ an effective polarization potential (see Sec. II B).

The scattering function $F_k(\vec{r})$ is further expanded in spherical harmonics to yield the usual body-frame coupled radial differential equations,

$$\left(\frac{d^2}{dr^2} - \frac{l(l+1)}{r^2} - 2V_{ll}^{(m)}(r) + k^2\right)u_{ll_0}^{(m)}(r) = 2\sum_{l' \neq l} V_{ll'}^{(m)}(r)u_{l'l_0}^{(m)}(r), \tag{2.5}$$

where $V_{ll'}^{(m)}(r)$ is the matrix element $\langle lm|V(\vec{r})|l'm\rangle$, and l_0 is a solution index which denotes the initial channel. These equations separate according to the irreducible representations of the symmetry group of the electron plus molecule Hamiltonian (for the target in a linear nuclear configuration), yielding sets of equations which can be described by the symmety of the system, e.g.,

Σ_g: $m = 0$, $l = 0, 2, 4, \ldots$,

Σ_u: $m = 0$, $l = 1, 3, 5, \ldots$,

Π_g: $m = 1$, $l = 2, 4, 6, \ldots$,

Π_u: $m = 1$, $l = 1, 3, 5, \ldots$.

The radial wave functions satisfy the usual scattering boundary conditions,

$$u_{ll_0}^{(m)}(0) = 0, \tag{2.6a}$$

$$u_{ll_0}^{(m)}(r) \underset{r\to\infty}{\sim} \delta_{ll_0}\sin(kr - l\tfrac{1}{2}\pi) + K_{ll_0}^{(m)}\cos(kr - l\tfrac{1}{2}\pi), \tag{2.6b}$$

the latter of which defines the K matrix.

The coupling matrix elements $V_{ll'}^{(m)}(r)$ appearing in the coupled-channel equations (2.5) are evaluated by expanding the effective interaction potential $V(\vec{r})$ in Legendre polynomials as

$$V(\vec{r}) = \sum_{\lambda\ \text{even}} v_\lambda(r)P_\lambda(\cos\chi), \tag{2.7}$$

where χ is the azimuthal angle of the scattering electron in the body-fixed coordinate system. We note that since CO_2 belongs to the point group $D_{\infty h}$, only even-λ coefficients appear. Carrying out the indicated angular integration, we obtain

$$V_{ll'}^{(m)}(r) = (-1)^m[(2l+1)(2l'+1)]^{1/2} \times \sum_{\lambda\ \text{even}} \frac{1}{2\lambda+1} v_\lambda(r) \times C(ll'\lambda; 00)C(ll'\lambda; -m, m), \tag{2.8}$$

with $C(j_1 j_2 j_3; m_1 m_2)$ the Clebsch-Gordan coefficients.[38] In practice the summation in Eq. (2.8) runs to some upper limit, $\lambda_{\max}$.

B. Interaction potential

In our treatment, the effective electron-molecule interaction potential $V(\vec{r})$ which appears in Eq. (2.4) consists of three types of terms: (i) a static contribution, which we determine *ab initio*; (ii) an exchange contribution, which we approximate by a local (but energy dependent) function; and (iii) a polarization contribution, which we treat semiempirically. Thus we can write each expansion coefficient $v_\lambda(r)$ as $v_\lambda(r) = v_\lambda^{\text{st}}(r) + v_\lambda^{\text{ex}}(r) + v_\lambda^{\text{pol}}(r)$. As Sec. IV will indicate, we find that all three types of interaction are necessary to properly describe the physics of low-energy $e - CO_2$ collisions.

The static term is simply $\langle X^1\Sigma_g^+|V_{\text{int}}(\tau, \vec{r})|X^1\Sigma_g^+\rangle_\tau$. For the ground-state wave function in this integral we use the near-Hartree-Fock SCFMO function of Mclean and Yoshimine.[39] This wave function is constructed from a basis set of double-zeta quality[40] augmented to include polarization functions and corresponds to an electronic energy of -187.7073 a.u.

In order to determine the expansion coefficients due to the static contribution, $v_\lambda^{\text{st}}(r)$, we first expand the target molecular charge distribution in Legendre polynomials about the origin of coordinates, giving coefficients $a_\lambda(r)$. Then each potential-energy expansion coefficient $v_\lambda^{\text{st}}(r)$ is given by the sum of a nuclear contribution and an electronic contribution, i.e.,

$$v_\lambda^{\text{st}}(r) = v_\lambda^{\text{nuc}}(r) + v_\lambda^{\text{el}}(r), \tag{2.9}$$

where for CO_2,

$$v_\lambda^{\text{nuc}}(r) = -(6/r)\delta_{\lambda 0} - 16\,\rho_<^\lambda/\rho_>^{\lambda+1}, \tag{2.10a}$$

$$v_\lambda^{\text{el}}(r) = \frac{4\pi}{2\lambda+1}\int a_\lambda(r')\frac{r_<^\lambda}{r_>^{\lambda+1}}r'^2\,dr', \tag{2.10b}$$

with $\rho_< = \min(r, R_{O\text{-}C})$, $r_< = \min(r, r')$, etc., and

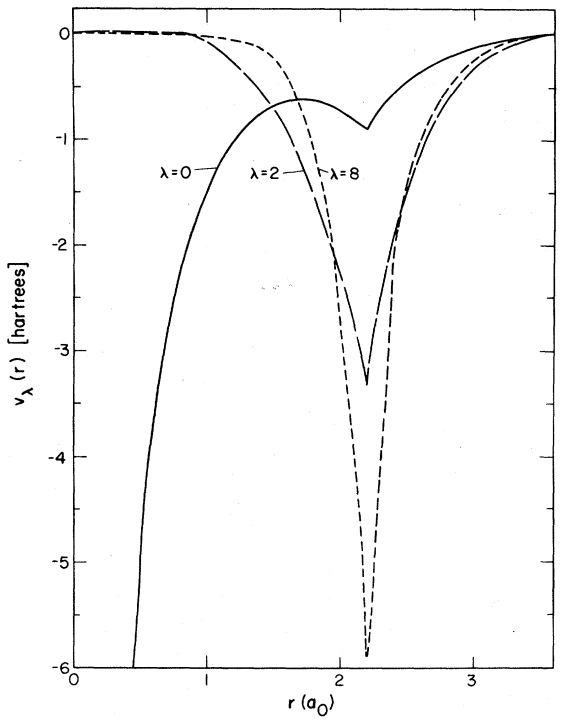

FIG. 1. Expansion coefficients $v_\lambda(r)$ in hartrees for the static e-CO_2 effective potential energy $V_{st}(\vec{r})$ for $\lambda=0$ (solid curve), $\lambda=2$ (dashed curve) and $\lambda=8$ (dotted curve). See Eq. (2.7).

$R_{O\text{-}C}$ the oxygen-carbon separation. The electronic contribution (2.10b) is evaluated by Gauss-Laguerre and Gauss-Legendre quadratures[41] using a cubic spline[42] to fit the mesh of points $a_\lambda(r)$. A few select $v_\lambda^{st}(r)$ are shown in Fig. 1.

The conventional procedure for treating an aspherical potential is to determine and include more and more coefficients $v_\lambda^{st}(r)$ until the cross sections obtained from the scattering calculation have converged. For CO_2, a different strategy is required. As λ increases, the nuclear contribution to a particular $v_\lambda^{st}(r)$ completely dominates the corresponding electronic term.[43] However, a large number of the *former* are necessary, since the convergence in spherical polar coordinates to the Coulomb singularities at the oxygen centers is quite slow. This poses no practical difficulty since any number of nuclear terms can be quickly computed from the analytic form (2.10a). We find that it is sufficient to include 15 electronic terms to satisfy our convergence criteria on the cross sections (see Sec. IV) but that 40 nuclear terms are required.

As a partial check on the accuracy of our static potential, we have extracted the permanent quadrupole moment from the asymptotic form

$$v_2^{st}(r) \underset{r\to\infty}{\sim} -q/r^3$$

obtaining $q=-3.8598ea_0^2$, which compares favorably with the theoretical value $q=-3.9086ea_0^2$ of Vučelić *et al.*[44] and the experimental value $q=-3.2014ea_0^2$ of Buckingham.[45] In the calculations reported in Sec. IV, we used our value for q in the long-range region.

The rigorous inclusion of exchange in eigenfunction expansion formulations of electron-molecule scattering theory (by antisymmetrizing the system wave function) leads to coupled integro-differential equations[37] rather than the coupled *differential* equations of (2.5). The solution of the resultant problem is difficult even for comparatively small diatomics.[4] Given the rather formidable computational problems attendant on the solution of the *static* problem in e-CO_2 scattering, we elected to seek a simpler (albeit approximate) way to account for the effects of exchange.

Stimulated in part by recent studies of electron-atom scattering,[46] we chose to consider a local energy-dependent exchange potential based on a free-electron gas model. Such an approach treats the electrons as a collection of noninteracting fermions and is analogous to the free-electron approximation of solid-state physics.[47]

The only application to date of such an exchange potential to *low-energy* electron-molecule scattering is that of Hara,[48] who studied $e-H_2$ collisions in this approximation with some success.[49] Our potential is analogous to his, although we do not spherically average the charge distribution. Thus we use an exchange potential of the form

$$V_{ex}(\vec{r}) = -(2/\pi)k_F(\vec{r})F(\eta), \tag{2.11}$$

where $k_F(\vec{r})$ is a Fermi wave vector (for the target) defined as

$$k_F(\vec{r}) = [3\pi^2\rho(\vec{r})]^{1/3}, \tag{2.12}$$

$\rho(\vec{r})$ being the ground-state charge distribution. In further explication of Eq. (2.11), the function $F(\eta)$ is given by

$$F(\eta) = \frac{1}{2} + \frac{1-\eta^2}{4\eta}\ln\left|\frac{1+\eta}{1-\eta}\right|, \tag{2.13a}$$

where

$$\eta = \eta(\vec{r}) = \frac{k_F(\vec{r})}{K(\vec{r})}, \quad K^2(\vec{r}) = k_F^2(\vec{r}) + (k^2+I), \tag{2.13b}$$

k^2 being the scattering energy (in Rydbergs) and I the ionization potential. We use[50] $I=1.0135$ Ry. The quantity $K(\vec{r})$ can be usefully interpreted as a "local wave number." The form of $V_{ex}(\vec{r})$ here defined gives a short-range attractive potential. We expand this potential in Legendre polynomials [using the coefficients $a_\lambda(r)$ determined in the calculation of $V_{st}(\vec{r})$] and add the resultant coefficients $v_\lambda^{ex}(r)$ to $v_\lambda^{st}(r)$ for $\lambda=0, 2, \ldots, 28$, thereby augment-

ing each electronic static term.

The final type of interaction we must take into account is the induced polarization of the target molecule by the incident electron. We chose to incorporate this into the problem making the usual adiabatic approximation,[51] which has been used extensively in low-energy electron-diatomic molecule scattering calculations.[4,52,6] Thus, rather than include closed electronic channels to introduce polarization effects, we augment the potential energy with terms having the correct asymptotic behavior and cut off at small r, i.e.,

$$V_{\rm pol}(\vec{r}) = \left(-\frac{\alpha_0}{2r^4} - \frac{\alpha_2}{2r^4} P_2(\cos\theta)\right) C(r), \qquad (2.14)$$

where α_0 is the spherical (isotropic, or average) polarizability, α_2 the nonspherical polarizability, and $C(r)$ a cutoff function defined by

$$C(r) = 1 - \exp[-(r/r_c)^6]. \qquad (2.15)$$

Finally, r_c is the single parameter in our treatment, the cutoff radius. The manner in which r_c was determined will be discussed in Sec. IV. For CO_2, we use[53] $\alpha_0 = 17.90$ a.u. and $\alpha_2 = 9.19$ a.u.

Thus, three models of the electron-molecule collision can be defined: (i) the *static* model (S), where $V(\vec{r}) = V_{\rm st}(\vec{r})$; (ii) an approximate *static-exchange* model (SE), where $V(\vec{r}) = V_{\rm st}(\vec{r}) + V_{\rm ex}(\vec{r})$; and (iii) an approximate *static-exchange with polarization* model (SEP), where

$$V(\vec{r}) = V_{\rm st}(\vec{r}) + V_{\rm ex}(\vec{r}) + V_{\rm pol}(\vec{r}).$$

We have studied $e - CO_2$ scattering in all three models (see Sec. IV).

C. Cross sections

We have determined three types of cross sections: (i) integrated total σ, (ii) momentum transfer $\sigma^{\rm mom}$, and (iii) differential $d\sigma/d\Omega$ in the theoretical context defined above. All are calculated from the K matrix, which was introduced in Eq. (2.6b) and is related to the S and T matrices via[54]

$$\underline{S} = (\underline{1} + i\underline{K})(\underline{1} - i\underline{K})^{-1} \qquad (2.16)$$

$$\underline{T} = \underline{1} - \underline{S}. \qquad (2.17)$$

In terms of the body-frame T matrix, the integrated total cross section for elastic scattering plus rotational excitation at energy k^2 is given by[5]

$$\sigma = \frac{\pi}{k^2} \sum_{ll'm} |T^m_{ll'}|^2, \qquad (2.18)$$

where, in practice, one includes only enough terms to converge σ.

A formula for the differential cross section can be obtained by squaring the body-frame fixed-nuclei scattering amplitude, transforming to a space-fixed coordinate system, and subsequently averaging over the Euler angles which define the orientation of the target with respect to the space-fixed axes.[5] The result can be written in a form convenient for computation as

$$\frac{d\sigma}{d\Omega} = \frac{1}{4k^2} \sum_{L=0}^{L_{\rm max}} d_L P_L(\cos\theta), \qquad (2.19)$$

where θ is the azimuthal angle of the scattering electron referred to the space-fixed axes and where d_L is given by

$$d_L = \frac{1}{2L+1}\left(\sum_{i=1}^{N} C^L_{ii} J_{ii} + 2\sum_{i=1}^{N-1}\sum_{j>i} C^L_{ij} J_{ij}\right), \qquad (2.20)$$

with

$$J_{ij} = R_i R_j + I_i I_j, \qquad (2.21)$$

where

$$\underline{T} = \underline{R} + i\underline{I}, \qquad (2.22)$$

and with

$$C^L_{ij} = [(2l_i+1)(2l'_i+1)(2l_j+1)(2l'_j+1)]^{1/2} \times C(l_i\, l_j\, L; 00) C(l'_i\, l'_j\, L; 00) \times C(l_i\, l_j\, L; -m_i, m_j) C(l'_i\, l'_j\, L; -m_i, m_j). \qquad (2.23)$$

The index i labels a set of quantum numbers (l_i, l'_i, m_i) corresponding to T-matrix element $T^{m_i}_{l_i l'_i}$, and N in Eq. (2.20) is the number of such elements needed for convergence. Finally, the allowed values of L are restricted by the condition

$$\max(|l_i - l_j|, |l'_i - l'_j|) \le L \le \min(l_i + l_j, l'_i + l'_j), \qquad (2.24)$$

and $L_{\rm max}$ is determined by the number of partial waves included in the calculations as $L_{\rm max} = 2l_{\rm max}$, where $l_{\rm max}$ is the largest-order partial wave needed for convergence. For a molecule with a center of symmetry, we also have the restrictions $l_i + l_j + L$ = even, $l'_i + l'_j + L$ = even, and the triangle relations $\Delta(l_i\, l_j\, L)$ and $\Delta(l'_i\, l'_j\, L)$.

In terms of the coefficients d_L, the total cross section becomes

$$\sigma = 2\pi \int_0^{\pi} (d\sigma/d\Omega) \sin\theta\, d\theta = (\pi/k^2)\, d_0, \qquad (2.25)$$

and the momentum-transfer cross section can be written

$$\sigma^{\rm mom} = 2\pi \int_0^{\pi} (1 - \cos\theta)(d\sigma/d\Omega) \sin\theta\, d\theta = \sigma - (\pi/3k^2)\, d_1. \qquad (2.26)$$

Equations (2.20), (2.25), and (2.26) were used in calculating the results reported in Sec. IV.

III. COMPUTATIONAL CONSIDERATIONS (REF. 33)

In order to solve the coupled differential equations (2.5), we choose to adapt the standard integral equations (IE) algorithm[32,55] to our problem. This is an efficient, rather stable algorithm, which in its simplest form reduces the solution to a series of step-by-step integrations from $r=0$ to the asymptotic region, avoiding matrix inversion. For small diatomic targets, one can simply apply the algorithm as it is usually presented (in fact, we have done so for low-energy $e-H_2$ scattering to verify our codes and procedures). However, when working with systems with highly anisotropic interaction potentials (e.g., $e-CO_2$) considerable modification of the algorithm must be made to avoid serious numerical errors; if these adaptations are ignored, spurious results obtain. We begin by briefly reviewing the theory and use of the standard IE techniques and thereby establish notation.

In matrix form, the coupled equations (2.5) for N channels can be written

$$\left(\frac{d^2}{dr^2}-\underline{L}(r)+\underline{k}^2\right)\underline{u}^{(m)}(r)=\underline{U}^{(m)}(r)\underline{u}^{(m)}(r), \tag{3.1}$$

where $\underline{U}^{(m)}(r)$ is an $N\times N$ potential-energy matrix, the ll' element of which is $2V_{ll'}^{(m)}(r)$, $\underline{L}(r)$ is an $N\times N$ diagonal matrix of the centrifugal barrier potential energy, with ll' element $[l(l+1)/r^2]\delta_{ll'}$, and where $\underline{k}^2=k^2\underline{1}$ is an $N\times N$ diagonal "energy matrix." The wave-function matrix $\underline{u}^{(m)}(r)$ is also an $N\times N$ matrix, the columns of which correspond to the N linearly independent solutions of (2.5).

We can convert Eq. (3.1) into an integral equation, obtaining

$$\underline{u}^{(m)}(r)=\underline{G}^1(r)-\int_0^r \underline{G}^{21}(r|r')\underline{U}^{(m)}(r')\underline{u}^{(m)}(r')\,dr' - \int_r^\infty \underline{G}^{12}(r|r')\underline{U}^{(m)}(r')u^{(m)}(r')\,dr', \tag{3.2}$$

where

$$\underline{G}^{ij}(r|r')=G^i(r)\underline{G}^j(r'), \tag{3.3}$$

with

$$[\underline{G}^1(r)]_{ll'}\equiv\hat{j}_l(kr)\delta_{ll'}, \tag{3.4a}$$

$$[\underline{G}^2(r)]_{ll'}\equiv(1/k)\hat{n}_l(kr)\delta_{ll'}, \tag{3.4b}$$

$\hat{j}_l(kr)$ and $\hat{n}_l(kr)$ being the Ricatti-Bessel and -Neumann functions,[56] respectively.

The "physical solution," $\underline{u}^{(m)}(r)$ of Eq. (3.2) can be related to a homogenous solution, $\underline{u}^0(r)$, which solves a homogeneous Volterra equation of the second kind.[57] This homogeneous solution satisfies the integral equation

$$\underline{u}^0(r)=\underline{G}^1(r)\underline{I}^2(r)-\underline{G}^2(r)\underline{I}^1(r), \tag{3.5}$$

$$\underline{I}^i(r)=\underline{1}\delta_{i2}+\int_0^r \underline{G}^i(r')\underline{U}^{(m)}(r')\underline{u}^0(r')\,dr' \quad [i=1,2]. \tag{3.6}$$

Then the physical wave function, which actually solves Eq. (3.2), is related to $\underline{u}^0(r)$ by

$$\underline{u}^{(m)}(r)=\underline{u}^0(r)(1+C), \tag{3.7}$$

where

$$\underline{C}=[\underline{1}-\underline{I}^2(\infty)][\underline{I}^2(\infty)]^{-1}. \tag{3.8}$$

In fact, one need not compute $\underline{u}^{(m)}(r)$ to determine the K matrix, for

$$\underline{K}=\underline{k}^{-1/2}\underline{I}^1(\infty)[\underline{I}^2(\infty)]^{-1}\underline{k}^{-1/2}. \tag{3.9}$$

Computationally, it is convenient to evaluate the homogeneous solutions and the I^i matrices by quadrature, replacing the integrals in (3.6) with sums as

$$\underline{I}^i(r_{j-1})=\underline{1}\delta_{i2}\sum_{k=1}^{j-1}\underline{G}^i(r_k)\underline{U}^{(m)}(r_k)\underline{u}^0(r_k)w_k, \quad [i=1,2] \tag{3.10}$$

r_k and w_k being the appropriate quadrature points and weights.[41] Then for a second-order quadrature (e.g., the trapezoidal) we have

$$\underline{u}^0(r_j)=\underline{G}^1(r_j)\underline{I}^2(r_{j-1})-\underline{G}^2(r_j)\underline{I}^1(r_{j-1}), \tag{3.11}$$

and the solution $\underline{u}^0(r)$ can be developed *noniteratively*, since

$$\underline{I}^i(r_{j-1})=\underline{I}^i(r_{j-2})+\underline{G}^i(r_{j-1})\underline{U}^{(m)}(r_{j-1})\underline{u}^0(r_{j-1})w_{j-1}. \tag{3.12}$$

The K matrix is calculated using $\underline{I}^i(r_{max})$ rather than $\underline{I}^i(\infty)$, where r_{max} is in the asymptotic region, i.e., large enough that the cross sections are stable in the final integration point.

The mesh of r values over which the quadrature was carried out is (in units of a_0) 0.0 to 0.02 in steps of 0.001, 0.02 to 3.0 in steps of 0.01, 3.0 to 30.0 in steps of 0.1, and 30.0 to 120.0 in steps of 0.2. A trapezoidal-rule quadrature scheme was used.

In the generation of the homogeneous solution matrix $\underline{u}^0(r)$ via the IE algorithm, it is possible for the solutions (the columns of $\underline{u}^0$) to become linearly dependent due to numerical inaccuracies. To resolve this problem a procedure called *stabilization* has been developed.[58] This entails decomposing the homogeneous solution at a particular value r_j where we choose to stabilize into the product of upper- and lower-triangular matrices. The solution matrix is replaced by the resultant upper-triangular matrix, the columns of which are guar-

anteed to be linearly independent. We find for $e - CO_2$ scattering that one must stabilize frequently at small r_j to avoid linear dependence; we stabilize every six integration points out to $r = 4.0a_0$.

For very large numbers of partial waves, stabilization is not sufficient to develop accurate solutions, for a further problem beyond linear dependence arises. Severe numerical difficulties obtain because the homogeneous solution which we are developing [via Eq. (3.5)] mixes "physical" channels corresponding to large- and small-l partial waves, leading to loss of significance at small r_j in important elements of the I^i matrices of Eq. (3.10).

To resolve this problem, we apply a *transformation procedure* to the developing homogeneous solution, applying a constant transformation $\underline{D}$ to $\underline{u}^0(r_{\text{trans}})$, where r_{trans} is a radius where we choose to transform, and to $\underline{I}^i(r_{\text{trans}})$, viz.,

$$\bar{\underline{u}}(r) = \underline{u}^0(r)\underline{D}, \quad \bar{\underline{I}}^i(r) = \underline{I}^i(r)\underline{D} \text{ at } r = r_{\text{trans}}. \tag{3.13}$$

We develop the solution for $r > r_{\text{trans}}$ as

$$\bar{\underline{u}}(r_j) = \underline{G}^1(r_j)\,\bar{\underline{I}}^2(r_{j-1}) - \underline{G}^2(r_j)\,\bar{\underline{I}}^1(r_{j-1}). \tag{3.14}$$

The K matrix obtained via Eq. (3.9) with either singly or multiply transformed I^i matrices is equal to that calculated with untransformed matrices, so this procedure is not an approximation.

The ideal choice for the constant transformation $\underline{D}$ would be $[\underline{I}^2(\infty)]^{-1}$, since this would give us $\underline{u}^{(m)}(r_{\text{trans}})$, thereby directly addressing the problem raised above. This is clearly impractical, however, so we use

$$\underline{D} = [\underline{I}^2(r_{\text{trans}})]^{-1}. \tag{3.15}$$

Depending on the number of partial waves involved, it may be sufficient to transform only once at some small-r integration point. In our problem, however, we have as many as 32 channels for certain symmetries and energies, corresponding to partial waves of order 0 to 62. In such extreme cases, repeated transformations in the region of the target are necessary. We transform every seven points out to $r = 4.0a_0$ in the results presented in Sec. IV, which are converged in frequency of transformation.

In point of fact, most of the partial waves required for convergence do not contribute to the cross section asymptotically. Thus $T^0_{28,30}$ is so small that it makes a completely insignificant contribution to σ in Eq. (2.18). This is a consequence[59] of the presence of the centrifugal barrier terms $l(l+1)/r^2$ in the scattering equations. Thus high-l channels carry no flux into the asymptotic region, although they do couple at smaller r and cannot be completely neglected. (This fact is the basis of pseudo bound state[9] and related approaches.[10])

To take advantage of this fact, we *truncate* all partial waves with $l \geq l_t$ at some *truncation radius* r_t chosen to be well beyond the region of the nuclear singularities. To do so, we first transform at $r = r_t$ according to Eq. (3.13) with $\underline{D} = [\underline{I}^2(r_t)]^{-1}$ and then delete the appropriate (large l) channels. The choice of r_t and l_t depends on the symmetry under consideration and the energy range of interest. For all symmetries studied (Σ_g, Σ_u, Π_g, Π_u), we use a truncation radius of $r_t = 4.0a_0$ to achieve convergence in this parameter. We find that it is sufficient to retain five partial waves beyond $r_t = 4.0a_0$ except in the Π_g symmetry, for which $l_t = 16$ is required for convergence in l_t. The mixing of the partial waves we have retained will be discussed in Sec. IV.

The truncation procedure is an approximation, albeit a very good one provided care is exercised in the choice of r_t and l_t. Although it saves considerable time in the solution of the coupled equations, this procedure is not mandatory.[60] We should emphasize that, in contrast, it is necessary to stabilize *and* to use the transformation procedure (or its equivalent) if these equations are to be solved using the IE or related algorithms. In addition, care must be taken in the evaluation of the spherical Bessel functions[61] and the Clebsch-Gordan coefficients[62] required for the solution of the problem, because large orders (l) are involved. Further details of the various numerical procedures employed can be found in Ref. 33.

IV. RESULTS

Using the procedure defined in Secs. II and III, converged total and momentum-transfer cross sections were calculated including all symmetries arising from $m = 0$ and $m = 1$ (i.e., Σ_g, Σ_u, Π_g, and Π_u). Contributions due to $m > 1$ (e.g., Δ_g) were found to be much smaller over the energy range studied than those for $m \leq 1$. This is consistent with the fact the effective potential $2V^{(m)}_{ll}(r) + l(l+1)/r^2$ becomes more purely repulsive as m is increased.[63]

In Sec. II., we indicated that a large number of electronic and nuclear expansion coefficients of the static interaction potential energy are required to converge the cross sections. Because of this fact, a large number of partial waves (channels) must be included to converge the results. To suggest the convergence behavior typical of this problem,[64] we present in Table I cross sections in the static approximation for $k^2 = 0.05$ Ry including only four expansion coefficients $v^{\text{st}}_\lambda(r)$. In these calculations N_{cc}, the number of coupled channels, ranges from

TABLE I. Convergence behavior of e-CO_2 cross sections with increasing number of partial waves in the static approximation "corrected" to remove the long-range quadrupole interaction (see text). Cross sections are shown in a_0^2 for a scattering energy $k^2 = 0.05$ Ry. Four expansion coefficients $V(\tilde{r})$ are included: $\lambda = 0$, 2, 4, 6. The maximum order of partial waves included in each case is l_{max}. The corresponding number of coupled channels is N_{cc}.

l_{max}	2	4	6	8	10	12	14	16
N_{cc}	2	3	4	5	6	7	8	9
Σ_g	5.2278	86.7671	76.1237	69.8322	68.7291	68.4519	68.3818	68.3717
Σ_u	0.0776	0.0111	0.0006	0.0008	0.0018	0.0022	0.0028	0.0030
Π_g	3.2(–4)	4.5(–4)	0.0020	0.0329	1.1554	0.1119	0.0846	0.0812
Π_u	20.9103	59.8970	20.6928	5.8042	3.7624	3.3697	3.3027	3.2929
Δ_g	1.1(–4)	1.1(–4)	1.1(–4)	1.2(–4)	1.2(–4)	1.2(–4)	1.2(–4)	1.2(–4)
Δ_u	1.0(–8)	1.0(–8)	1.0(–8)	1.1(–8)	1.1(–8)	1.1(–8)	1.1(–8)	1.1(–8)
Total	26.2162	146.6760	96.8193	75.6703	63.6490	71.9359	71.7716	71.7784

2 to 9. (The final converged cross section for this case is $71.7449 a_0^2$.) In order to focus on the convergence characteristics of the *short-range* interaction, we here remove the long-range quadrupole contribution from $v_2^{st}(r)$ by adding to it a "correction term" of the form $v_2^{corr}(r) = +qr^{-3}C(r)$, where $C(r)$ is given by Eq. (2.15) with $r_c = 4.0 a_0$. Thus we replace $v_2^{st}(r)$ with $v_2^{st}(r) + v_2^{corr}(r)$. The convergence behavior in λ_{max} is illustrated in Table II, where we show cross sections in this model which are converged in partial waves to $< 1\%$. Also shown is the number of channels required to satisfy this criterion.

Throughout these calculations, we used cross sections as indicators of convergence. A number of authors use eigenphase sums for this purpose,[6,35] where the eigenphases are determined by diagonalizing the K matrix for the symmetry under consideration and taking the arctangent of the resulting eigenvalues. Although useful as indicators that convergence is at hand, we have found that at low energies a small difference in two eigenphases (say, 2%) can correspond to a fairly large difference in the corresponding cross sections (>10%), since the contribution to σ from a particular eigenphase η_{lm} is $(4\pi/k^2)\sin^2\eta_{lm}$.

The addition of exchange and polarization interactions only marginally affects the number of channels required for convergence. In general, we find that the "bonding symmetries" (Σ_g, Π_u, etc.) converge more slowly than do the "nonbonding" symmetries (Σ_u, Π_g, etc.), and that cross sections in the Σ_g symmetry, which reflect the full static potential for the s-wave ($l = 0$) channel, are the most difficult to converge. The final number of channels included in these calculations is 32 for Σ_g, 15 for Σ_u and Π_g, and 23 for Π_u near resonance, 15 for Π_u far from resonance. We integrate to $r_{max} = 120 a_0$ in all three approximations (S, SE, and SEP).

In the SEP approximation, we must select a value for the cutoff parameter in the polarization potential, r_c defined in Eq. (2.15). In order to do this,

TABLE II. Convergence behavior of e-CO_2 cross sections (in a_0^2) with λ_{max}, the maximum-order expansion coefficient included in $V(\tilde{r})$ [see Eq. (2.7)]. The static approximation is made with the long-range quadrupole deleted (see text). All cross sections are converged in number of partial waves (l_{max}) to $\leq 1\%$. N_{cc} is the number of channels required to satisfy this criterion.

λ_{max}	2	4	6	8	10	12	14	16	18
Σ_g	48.8966	94.1177	68.3702	59.6961	54.7470	51.6689	49.7088	48.4416	47.6084
Σ_u	0.3159	0.0520	0.0030	0.1045	0.4805	2.0771	25.8069	20.4357	3.2939
Π_g	0.0739	9.5032	0.0867	0.3476	0.0689	0.0102	0.0045	0.0029	0.0022
Π_u	7.3529	4.6366	3.2916	4.0311	7.7086	17.6299	40.9668	89.5212	174.3648
Δ_g	7.4(–5)	1.4(–4)	1.2(–4)	1.2(–4)	1.2(–4)	1.1(–4)	1.1(–4)	1.1(–4)	1.1(–4)
Δ_u	8.4(–7)	8.5(–8)	1.1(–8)	1.0(–8)	1.0(–8)	1.0(–8)	1.0(–8)	1.0(–8)	1.0(–8)
Total	56.6392	108.3100	71.7449	64.1796	63.0052	71.3862	116.4872	158.4016	225.2694
N_{cc}	6	9	11	13	15	17	18	20	20

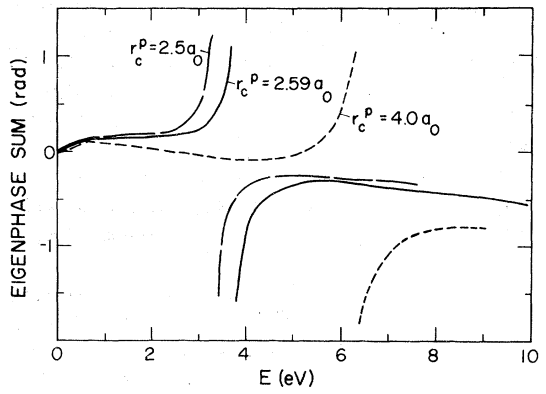

FIG. 2. Converged eigenphase sums for e-CO_2 scattering in the Π_u symmetry in the SEP model using the HFEGE potential. Three cutoff parameters [r_c in Eq. (2.15)] are shown: $r_c = 2.5a_0$ (dashed curve) $r_c = 4.0a_0$ (dotted curve) and $r_c = 2.59a_0$ (solid curve). The latter choice produces a Π_u shape resonance at 3.8 eV.

we have "tuned" the potential so as to position the well-known Π_u resonance peak at 3.8 eV. This requires a value of $r_c = 2.59a_0$. This choice uniquely defines the SEP potential energy which we use for scattering from 0.07 to 10.0 eV. It should be pointed out that the value of the resonance energy is rather sensitive to the choice of the cutoff radius, as shown in Fig. 2, where the Π_u eigenphase sums are graphed for three cases: $r_c = 2.5a_0$ (dashed curve), $r_c = 2.59a_0$ (solid curve), and $r_c = 4.0a_0$ (dotted curve).

Converged total cross sections at several energies in the SEP model appear in Table III and are graphed in Fig. 3. The numbers in parenthesis are the corresponding eigenphase sums. We show both the cross sections in Σ_g, Σ_u, Π_g, Π_u symmetries and their sum, σ. The total cross section has a peak value at the resonance energy (3.8 eV) of $110.2565a_0^2$. The width of the resonance is ~0.5 eV.

As Fig. 3 demonstrates, at low energies the Σ_g contribution completely dominates the total cross section. Similarly, in the vicinity of the resonance, Π_u is the dominant symmetry. At other energies, Σ_u contributions become quite important. It should be noted that although we "tune" the polarization potential in the Π_u symmetry (at 3.8 eV), we use the resultant form in energy ranges where other symmetries are much more significant. We also see that, consistent with the effective potential arguments mentioned earlier, the Π_g cross sections are by far the smallest of the four here presented.

To further analyze these cross sections, it is useful to investigate the extent to which the various partial waves that contribute to the cross section mix in the asymptotic region. For low-energy electron collisions with some smaller targets, this mixing is often not appreciable, and one can usefully think about the scattering in terms of individual partial waves. However, for CO_2 this is not generally the case. This point is illustrated in Fig. 4, which shows the contribution to the scattering over the energy range studied of the two lowest $-l$ partial waves in Σ_g, Σ_u, and Π_u symmetries.[65]

TABLE III. Converged integrated cross sections (in a_0^2) for e-CO_2 in the SEP model using the HFEGE and a polarization cutoff $r_c = 2.59a_0$. The corresponding eigenphase sums are shown (in rad) in parentheses. The parameters required for convergence are described in the text.

E(eV)	0.07	0.1	0.5	1.0	2.0	3.0	3.5
Σ_g	226.7339	179.4213	37.9246	15.1480	6.8633	5.1104	4.6909
	(0.2927)	(0.3120)	(0.2982)	(0.2279)	(0.1050)	(−0.0092)	(−0.0637)
Σ_u	3.7153	3.4513	3.8029	6.0101	10.5967	13.9785	15.1616
	(−0.0444)	(−0.0523)	(−0.1201)	(−0.2043)	(−0.3695)	(−0.5155)	(−0.5802)
Π_g	0.2106	···	0.1148	···	0.1136	···	0.0948
	(−0.0068)	···	(−0.0096)	···	(−0.0013)	···	(−0.0198)
Π_u	9.5901	10.6070	12.6696	9.3535	4.6191	6.7117	30.5329
	(0.0377)	(0.0479)	(0.1225)	(0.1518)	(0.1546)	(0.2291)	(0.5641)

E(eV)	3.8	4.0	5.1	5.9	8.0	10.0
Σ_g	4.5012	4.3939	3.9877	3.8261	3.8702	5.3371
	(−0.0953)	(−0.1157)	(−0.2170)	(−0.2754)	(−0.3405)	(−0.2509)
Σ_u	15.7306	16.0546	17.1792	17.4502	16.8578	15.4439
	(−0.6167)	(−0.6400)	(−0.7552)	(−0.8269)	(−0.9781)	(−1.0905)
Π_g	0.1146	0.1332	0.3106	0.5096	1.2089	1.9802
	(−0.0259)	(−0.0315)	(−0.0566)	(−0.0775)	(−0.1318)	(−0.1763)
Π_u	89.9101	45.3868	4.7014	3.7754	4.6436	5.8722
	(−1.5736)	(−0.8611)	(−0.3377)	(−0.3356)	(−0.4236)	(−0.5236)

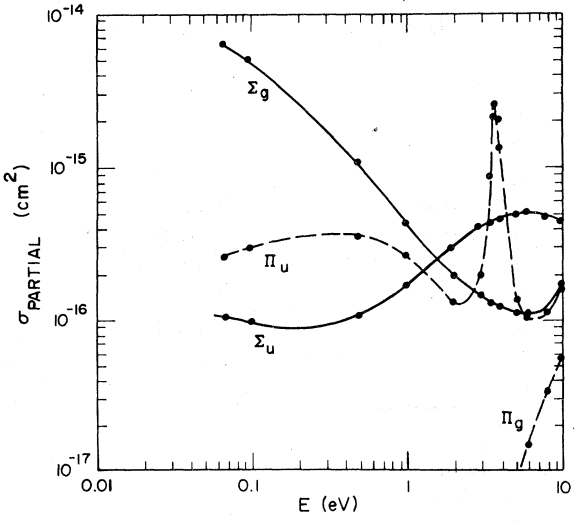

FIG. 3. Converged integrated cross sections for e-CO_2 scattering in Σ_g, Σ_u, Π_g, and Π_u symmetries in the SEP model using the HFEGE potential and a polarization cutoff radius $r_c = 2.59a_0$. The Π_u resonance energy is 3.8 eV.

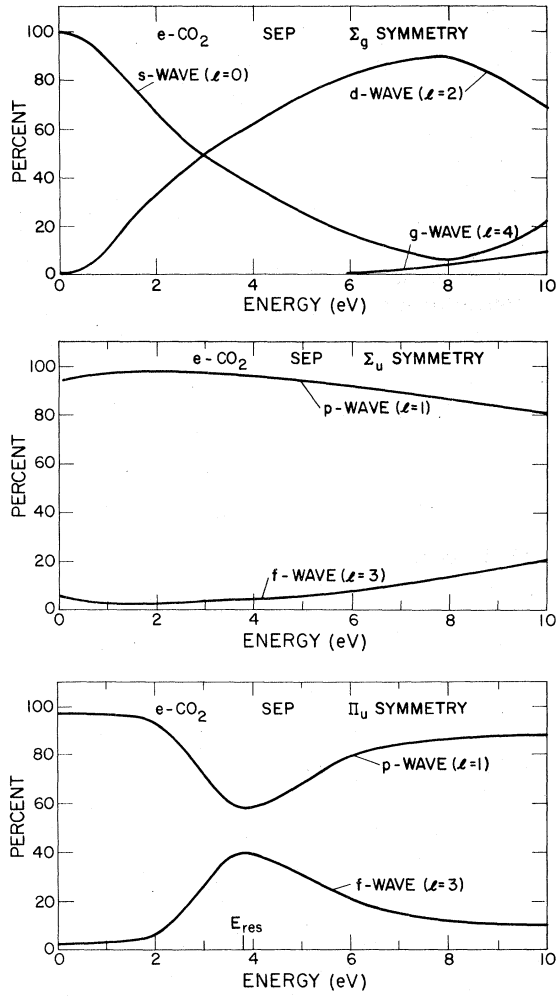

FIG. 4. Asymptotic mixing of partial waves for e-CO_2 scattering in Σ_g, Σ_u, and Π_u symmetries in the SEP approximation defined in the text. The vertical axis shows the percentage of the scattering in the symmetries considered due to each partial wave (Ref. 65).

We find that while Σ_u scattering is essentially pure p wave over the whole energy range, Σ_g is s wave at low energies ($\lesssim$1 eV), s and d wave at intermediate energies (1–8 eV) and predominantly d-wave at higher energies (8–10 eV). The Π_u resonance is characterized by a mixture of p and f waves, while scattering in this symmetry far from resonance is predominantly p wave.

The first experimental studies of the angular distributions for e-CO_2 collisions near the 3.8-eV resonance incorrectly ascribed it to s wave.[24] Subsequently, Danner[66] and Spence *et al.*[23] observed that resonant scattering is predominantly but not totally p wave in character. This conclusion is supported by our calculations.

It is the enormous s-wave Σ_g cross sections obtained for energies smaller than 0.1 eV that are responsible for the anomalously large momentum-transfer cross sections observed by Phelps *et al.* In Fig. 5, we compare our values for σ^{mom} to the experimental results of Lowke, Phelps, and Irwin[20]; comparisons at several energies are presented in Table IV. We shall discuss possible interpretations of these findings in Sec. V.

We also calculated differential cross sections $d\sigma/d\Omega$ [using Eq. (2.19)] for several energies in the SEP approximation. Reliable theoretical calculations of differential cross sections require a greater degree of accuracy in the scattering wave function than is needed to determine total or momentum-transfer cross sections, because $d\sigma/d\Omega$ is more sensitive to interference among off-diagonal T-matrix elements. In Fig. 6, we show results for angles from 0° to 180° at three scattering energies, 0.07, 4.0, and 10.0 eV. The behavior of the differential cross section at 0.07 eV is typical of energies $\lesssim$0.5 eV, and that of the 10.0-eV result is typical of energies from ~5.0 to 10.0 eV, the forward peaking becoming more pronounced as energy increases. The p-f character of the $^2\Pi_u$ resonance is clearly shown in $d\sigma/d\Omega$ at 4.0 eV, where this symmetry is dominant.

One frequently-used approach to the calculation of electron-molecule cross sections is the Born approximation[2] (BA). The partial-wave BA to the K-matrix (or T-matrix) elements $K^m_{ll'}$ (or $T^m_{ll'}$) *at low scattering energies* is expected to be reliable for l and l' sufficiently large, since the centrifugal barriers associated with these channels cause the

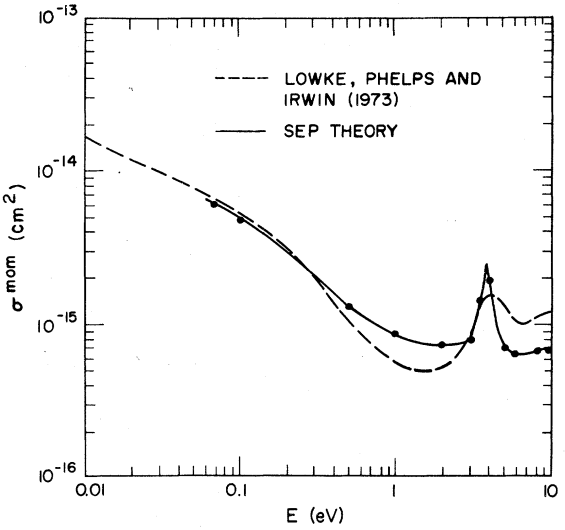

FIG. 5. Converged momentum-transfer cross sections for e-CO_2 scattering in the SEP model using the HFEGE potential with $r_c = 2.59a_0$ compared with experimental data extracted from swarm experiments (Ref. 20).

scattering to be weak. Clearly, for e-CO_2 collisions, we would not expect the BA to be valid for Σ_g scattering, since in this symmetry a very large contribution obtains from $l = l' = 0$.

In order to see where the BA does work for this application we have carried out a simple partial-wave Born analysis including long-range terms only, i.e., permanent quadrupole and induced polarization interactions. The relevant equations are briefly summarized in the Appendix, and the results for Σ_u, Π_g, and Π_u symmetries are given in Table V along with the SEP coupled-channel results for comparison. The BA appears to be successful only for the Π_g symmetry at low scattering energies. This is hardly surprising, since Π_g partial waves at low energy are excluded from the region of the strong static potential by the $l = 2$ centrifugal barrier. Even in cases where the BA clearly fails, e.g., Π_u symmetry at 3.0 eV, a study of individual T-matrix elements $T^m_{ll'}$ reveals that for large ll', the agreement between Born and coupled-channel results is good. However, these elements do not contribute significantly to the total cross section. The BA appears to be an unsatisfactory tool for calculation of the important contributions to the total e-CO_2 cross sections.

In Fig. 4, we illustrated the mixing of partial waves implicit in the SEP e-CO_2 wave functions. The relative importance of the off-diagonal elements of the K matrix to the total and momentum-transfer cross sections provides an indication of

TABLE IV. Converged theoretical total [$\sigma(T)$] and momentum-transfer [$\sigma^{mom}(T)$] cross sections in a_0^2 and Å^2 (in parentheses) for e-CO_2 scattering in the SEP approximation using the HFEGE potential and a polarization cutoff of $r_c = 2.59a_0$. Also shown are measured momentum-transfer cross sections $\sigma^{mom}(E)$ extracted from swarm experiments; see Ref. 20.

E(eV)	0.07	0.1	0.5	1.0	2.0	3.0	3.5	3.8	4.0	5.1	5.9	8.0	10.0
$\sigma(T)$	237.9836	194.6609	54.5459	30.5319	22.1906	25.8061	50.4730	110.2451	65.9660	26.1767	25.5627	26.5789	28.6318
	(66.6354)	(54.5050)	(15.2728)	(8.5489)	(6.2134)	(7.2257)	(14.1324)	(30.8686)	(18.4705)	(7.3295)	(7.1575)	(7.4421)	(8.0169)
$\sigma^{mom}(T)$	216.8731	173.5418	45.9881	30.7730	26.4095	28.4128	50.1233	111.1315	68.6035	24.9316	22.5867	21.6867	24.4773
	(60.7245)	(48.5917)	(12.8767)	(8.6164)	(7.3947)	(7.9556)	(14.0345)	(31.1168)	(19.2090)	(6.9808)	(6.3243)	(6.0723)	(6.8454)
$\sigma^{mom}(E)$	228.57	...	38.57	...	18.75	...	...	...	...	...	...	...	43.21
	(64.00)	...	(10.8)	...	(5.25)	...	...	...	...	...	...	...	(12.10)

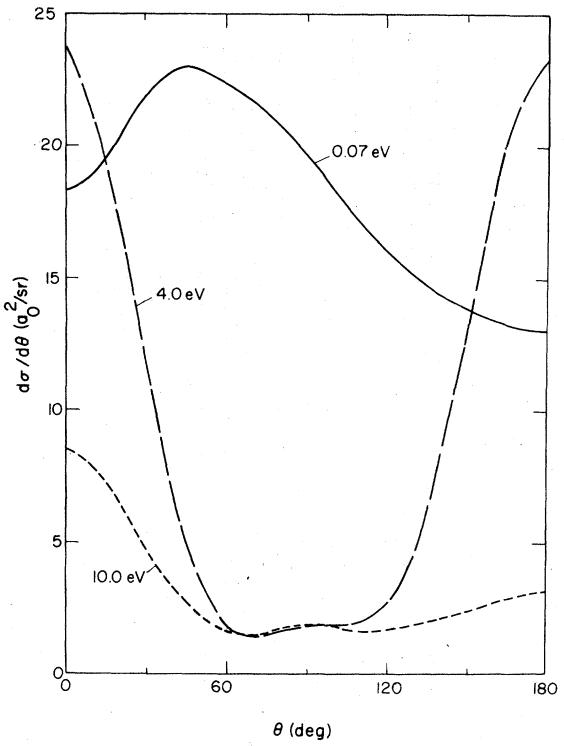

FIG. 6. Differential cross sections for e-CO_2 scattering in the SEP approximation with the HFEGE potential and a polarization cutoff of $r_c = 2.59a_0$ for 0.07 eV (solid curve), 4.0 eV (dashed curve), and 10.0 eV (dotted curve).

the importance of this mixing and can be examined by invoking an *asymptotic decoupling approximation* (ADA), wherein we retain the full partial-wave coupling (for $r > r_t$) out to the asymptotic region but there set $T^m_{ll'} = T^m_{ll}\delta_{ll'}$, in Eq. (2.18) for the total cross section. This approximation effectively decomposes the scattering into individual-l partial waves. [This is somewhat different from, say, pseudo-bound-state approaches,[9] which neglect *coupling* altogether in the exterior (long-range potential) region or the low-l spoiling approximation,[10] which neglects not only partial-wave mixing but the entire exterior region itself.] Results calculated in the ADA are shown in Table VI, which suggests that for purposes of calculating σ and $\sigma^{\rm mom}$, one can get *qualitatively* correct behavior (versus energy) in the ADA but that the neglect of the off-diagonal T-matrix elements considerably changes the value of these cross sections.

All results presented so far were obtained in a model which includes electrostatic, exchange, and polarization interactions. In order to study the importance of these various interactions, we have calculated total cross sections in the S and SE approximations defined in Sec. II B; the results are shown in Fig. 7. Note the presence of a spurious peak in $\sigma(S)$, which is due to a false resonance in Π_u symmetry. This disappears in the SE cross sections. In the model SE results, the 3.8-eV Π_u resonance (at ~8.0 eV) is broad and quite small. Once polarization is included, clear resonant behavior appears (in the eigenphases; see Table III), and we can position the peak at 3.8 eV. This achieved, the agreement of σ with experiment is satisfactory even at low energies, as shown in Fig. 6, which compares our SEP cross sections with the early measurements of Ramsauer and Kollath[15] and of Brüche.[16] These results suggest that within the context of our model of the electron-CO_2 interaction, all three types of interactions must be taken into account, especially if one is interested in scattering at low electron energies.

V. CONCLUSION

In this paper, we have reported converged total and momentum-transfer cross sections for e-CO_2 collisions calculated in the coupled-channel method for scattering energies from 0.07 to 10.0 eV. To our knowledge, this is the largest target (and the only polyatomic) that has been studied at this level of accuracy to date. Our results reproduce the

TABLE V. Electron-CO_2 scattering in the partial-wave Born approximation. Long-range permanent quadrupole and induced polarization interactions are taken into account (see Appendix). Cross sections are given in a_0^2, and converged coupled-channel cross sections (from Table III) are presented in parentheses for comparison.

E(eV)	0.07	0.1	0.5	1.0	2.0	3.0
Σ_u	2.7785	2.1083	0.3050	2.6969	10.3103	16.3992
	(3.7153)	(3.4513)	(3.8029)	(6.0101)	(10.5967)	(13.9785)
Π_g	0.1987	0.1760	0.1134	0.1922	0.4868	0.8550
	(0.2106)	...	(0.1148)	...	(0.1136)	...
Π_u	10.2075	11.7177	25.9399	37.8507	50.0600	52.5170
	(9.5901)	(10.6070)	(12.6696)	(9.3535)	(4.6191)	(6.7117)

TABLE VI. The asymptotic decoupling approximation (ADA) for e-CO_2 collisions. Full coupled-channel total [σ(CC)] and momentum-transfer [σ^{mom}(CC)] cross sections in a_0^2 calculated in the SEP model are compared with their counterparts in the ADA as defined in the text.

E(eV)	0.07	0.1	0.5	1.0	2.0	3.0	3.5	4.0	5.1	5.9	8.0	10.0
σ(CC)	237.9836	194.6609	54.5459	30.5319	22.1906	25.8061	50.4730	65.9660	26.1767	25.5627	26.5789	28.6318
(ADA)	235.6109	192.4727	51.7659	26.8862	17.2550	18.6227	30.9513	41.4058	21.3116	21.3184	21.8441	21.5499
σ^{mom}(CC)	216.8731	173.5418	45.9881	30.7730	26.4095	28.4128	50.1233	68.6035	24.9316	22.5867	21.6867	24.4773
(ADA)	211.3744	167.9891	38.8486	21.6921	16.2462	17.1868	28.5661	37.1253	16.7296	16.0825	16.0699	15.8613

low-energy experimental values for σ and σ^{mom} satisfactorily, indicating that although approximate, our model potential accurately reflects the principal features of the true e-CO_2 interaction.

It is true that our approach to exchange is rather crude; at best it appears to mock in some average sense the true effects of exchange. It is likely that a fully accurate static-exchange calculation on e-CO_2 would alter the quantitative SE results, perhaps giving a better representation of the $^2\Pi_u$ compound state than we obtain. We do not believe the low-energy results ($\lesssim$0.1 eV) would be significantly altered. It is further the case that because of the method we employed to determine the polarization cutoff radius, our polarization potential probably corrects to some extent the shortcomings of our exchange potential. Similar procedures for dealing with adjustable parameters have been employed by other authors who treat exchange approximately.[6,67] For example, in their studies of e-N_2 scattering, Burke and Chandra[6] approximate exchange effects by ignoring the exchange kernel term but explicitly enforcing orthogonality of the scattering orbital to core orbitals of the appropriate symmetry; they then introduce polarization as do we. However, in the e-N_2 scattering problem, there is no core π_g orbital, so polarization must completely adjust this symmetry to reproduce the $^2\Pi_g$ resonance at ~2.3 eV. In contrast, our exchange potential affects all symmetries, leaving a minor but important adjustment in the location (but not the existence) of the resonance peak to be made by polarization. A possibly useful alternate procedure would be to use a local-exchange potential and to orthogonalize[68] as

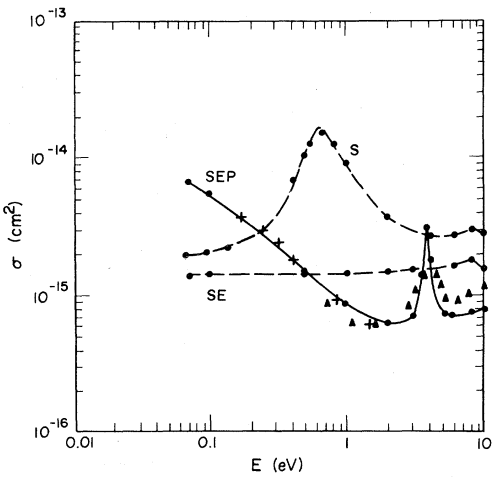

FIG. 7. Converged total integrated cross sections (including Σ_g, Σ_u, Π_g, and Π_u symmetries) for e-CO_2 scattering in the static (S), static-exchange (SE), and static-exchange-polarization (SEP) models. Experimental data: x, Ref. 15; Δ, Ref. 16.

do Burke and Chandra.[6,69] Such an approach would have the further advantage of allowing an estimate of the validity of the local potential used by seeing to what extent orthogonalization affects the results.

The neglect of vibrational channels in our calculation will probably be important only in the vicinity of the resonance, where significant vibrational excitation can take place. Inclusion of these channels is expected to broaden the resonance and reduce the peak value of the cross section.

By way of interpretation of our results, it is possible that the unusually large cross sections we calculate for $E < 0.1$ eV are reflecting a "virtual state"[54] (a zero of the S matrix on the positive imaginary k axis). At these energies, the scattering is almost purely s wave in the Σ_g symmetry, and there may be a nearly bound $l = 0$ state in the e-CO_2 potential.

The theory and computational procedures described above should be applicable to a wide variety of problems in electron-molecule collisions provided the target is closed shell and does not possess a stronger or more anisotopic electrostatic interaction potential than does CO_2. For calculation of total cross sections in electron-heteronuclear molecule collisions a frame transformation[6,70] to a laboratory frame would be required, but provided this is carried out beyond the truncation radius for the problem, this procedure should not be arduous.

ACKNOWLEDGMENTS

The authors would like to thank Dr. A. V. Phelps, Dr. James S. Cohen, and Dr. D. G. Truhlar for conversations about various aspects of this research. One of us (M.A.M.) gratefully acknowledges the Associated Western Universities for making his stay at Los Alamos Scientific Laboratory possible, and the staff of T-12 at LASL, especially Dr. David Cartwright and Dr. Barry Schneider, for assistance and computer time.

APPENDIX

The K matrix can be written in terms of the scattering wave function $\underline{u}^{(m)}$, which solves Eq. (3.2), as

$$\underline{K} = -\frac{1}{k}\int_0^\infty \underline{u}^B(r)^* \underline{U}^{(m)}(r)\underline{u}^{(m)}(r)\,dr, \tag{A1}$$

where $\underline{U}^{(m)}$ is defined in Sec. III and $\underline{u}^B(r)$ is the free-particle (or Born) undistorted wave-function matrix, with ij element

$$[\underline{u}^{(B)}(r)]_{ij} = \hat{j}_{l_i}(kr)\delta_{l_i l_j}. \tag{A2}$$

If we consider only long-range terms, then the averaged electron-molecule interaction potential, which is used to calculate $\underline{U}^{(m)}$ as in Eq. (2.8), is given by

$$V(\vec{r}) = -\frac{\alpha_0}{2r^4} - \left(\frac{\alpha_2}{2r^4} + \frac{q}{r^3}\right) P_2(\cos\theta). \tag{A3}$$

Substituting $\underline{u}^B(r)$ for $\underline{u}^{(m)}(r)$ in Eq. (1) gives an expression for the K matrix in the Born approximation. Using Eq. (A3) for $V(\vec{r})$, we obtain for the ll' element of $\underline{K}$,

$$K^m_{ll'} = k\alpha_0 R^{(2)}(ll')\delta_{ll'} + k\left(\frac{4}{5}\pi\right)^{1/2} I_2(ll'm)[\alpha_2 R^{(2)}(ll') + 2qR^{(1)}(ll')], \tag{A4}$$

where

$$I_\lambda(ll'm) = \int\int Y^m_l(\hat{r})^* Y^0_\lambda(\hat{r}) Y^m_{l'}(\hat{r})\,d\hat{r}. \tag{A5}$$

The radial integrals appearing in (A4) are found to be

$$R^{(1)}(ll') = \frac{\pi}{8}\left[n(n+1)\Gamma\left(\frac{l-l'+3}{2}\right)\Gamma\left(\frac{l'-l+3}{2}\right)\right]^{-1}, \tag{A6a}$$

$$R^{(2)}(ll') = \frac{\pi k}{4(2n-1)} \times \frac{\Gamma(n+\frac{1}{2})}{\Gamma(n+\frac{3}{2})\Gamma[\frac{1}{2}(l-l'+4)]\Gamma[\frac{1}{2}(l'-l+4)]}, \tag{A6b}$$

where we have introduced an integer

$$n = \tfrac{1}{2}(l+l'), \tag{A7}$$

and where the case $l = l' = 0$ is excluded. In the case $\alpha_0 = \alpha_2 = 0$, the diagonal elements of $\underline{K}$ are given by

$$K^m_{ll} = k\frac{q}{5}(-1)^m \frac{2l+1}{l(l+1)} C(ll2;00)C(ll2;m,-m). \tag{A8}$$

---

*Supported in part by the U.S. Energy Research and Development Administration, Division of Physical Research and by the Robert A. Welch Foundation.

†Fannie and John Hertz Foundation Fellow.

‡JILA Visiting Fellow. Permanent address: Dept. of Physics, Rice University, Houston, Tex. 77001.

[1]See reviews by D. E. Golden, N. F. Lane, A. Temkin, and E. Gerjuoy, Rev. Mod. Phys. 43, 642 (1971);

K. Takayanagi and Y. Itikawa, Adv. At. Mol. Phys. 6, 105 (1970).
[2]Cf. E. S. Chang, Phys. Rev. A 2, 1403 (1970); 10, 1911 (1974); Y. Itikawa, J. Phys. Soc. Jpn. 36, 1121 (1974).
[3]Cf. K. Takayanagi, J. Phys. Soc. Jpn. 20, 562 (1965); A. Dalgarno and R. J. W. Henry, Proc. Phys. Soc. Lond. 85, 679 (1965); T. N. Rescigno, C. W. McCurdy, Jr., V. McKoy, and C. F. Bender, Phys. Rev. A 13, 216 (1976).
[4]Cf. N. F. Lane and S. Geltman, Phys. Rev. 160, 53 (1967); R. J. W. Henry and N. F. Lane, *ibid.* 183, 221 (1969); R. J. W. Henry, Phys. Rev. A 2, 1349 (1970); Y. Itikawa, J. Phys. Soc. Jpn. 28, 1062 (1970); O. H. Crawford and A. Dalgarno, J. Phys. B 4, 494 (1971).
[5]Cf., P. G. Burke and A. L. Sinfailam, J. Phys. B 3, 641 (1970).
[6]P. G. Burke and N. Chandra, J. Phys. B 5, 1696 (1972).
[7]B. I. Schneider, Phys. Rev. A 11, 1957 (1975); B. I. Schneider and P. J. Hay, *ibid.* 13, 2049 (1976).
[8]T. N. Rescigno, C. W. McCurdy, Jr., and V. McKoy, Phys. Rev. A 10, 2240 (1974); 11, 825 (1975).
[9]M. A. Morrison and N. F. Lane, Phys. Rev. A 12, 2361 (1975).
[10]C. W. McCurdy, Jr., T. N. Rescigno, and V. McKoy, J. Phys. B 9, 691 (1976).
[11]E. Gerjuoy and S. Stein, Phys. Rev. 97, 1671 (1955); 98, 1848 (1955).
[12]C. W. McCurdy, Jr., and V. McKoy, J. Chem. Phys. 61, 2820 (1974).
[13]N. N. Sobolev and V. V. Sobovikov, *Invited Papers on the Proceedings of the Fifth International Conference on the Physics of Electronic and Atomic Collisions, Leningrad, 1967,* edited by L. Branscomb (Nauka, Leningrad, 1967), p. 47.
[14]C. J. Elliott, O. P. Judd, A. M. Lockett, and S. D. Rockwood, Los Alamos Scientific Laboratory Informal Report, LA-5562-MS, 1974 (unpublished); D. C. Tyte, Adv. Quantum Electron. 1, 129 (1970).
[15]C. Ramsauer and R. K. Kollath, Ann. Phys. (Leipz.) 83, 1129 (1927); R. K. Kollath, *ibid.* 15, 485 (1932).
[16]E. Brüche, Ann. Phys. (Leipz.) 83, 1065 (1927); see also, R. B. Brode, Rev. Mod. Phys. 5, 257 (1933).
[17]R. K. Tice and D. Kivelson, J. Chem. Phys. 46, 4748 (1967); see also, F. C. Fehsenfeld, *ibid.* 39, 1653 (1963).
[18]J. L. Pack, R. E. Voshall, and A. V. Phelps, Phys. Rev. 127, 2084 (1962).
[19]R. D. Hake, Jr. and A. V. Phelps, Phys. Rev. 158, 70 (1967).
[20]J. J. Lowke, A. V. Phelps, and B. W. Irwin, J. Appl. Phys. 44, 4664 (1973).
[21]A. Stamatovic and G. J. Schulz, Phys. Rev. 188, 213 (1969); M. J. W. Boness and G. J. Schulz, Phys. Rev. A 9, 1969 (1974); see also, M. J. W. Boness, J. B. Hasted, and I. W. Larkin, Proc. R. Soc. A 305, 493 (1968); A. Andrick, D. Danner, and H. Ehrhardt, Phys. Lett. 29A, 346 (1969); and P. D. Burrow and L. Sanche, Phys. Rev. Lett. 28, 333 (1972).
[22]M. J. W. Boness and J. B. Hasted, Phys. Lett. 21, 526 (1966).
[23]D. Spence, J. L. Mauer, and G. J. Schulz, J. Chem. Phys. 57, 5516 (1972).
[24]M. J. W. Boness and G. J. Schulz, Phys. Rev. Lett. 21, 1031 (1968).
[25]C. R. Claydon, G. A. Segal, and H. S. Taylor, J. Chem. Phys. 52, 3387 (1970). In connection with this work, see also M. Krauss and D. Neumann, Chem. Phys. Lett. 14, 26 (1972).
[26]J. N. Bardsley, J. Chem. Phys. 51, 3384 (1969).
[27]H. Lehning, Phys. Lett. 28A, 103 (1968); D. Andrick and F. H. Reed, J. Phys. B 4, 389 (1971).
[28]Y. Itikawa, Phys. Rev. A 3, 831 (1971).
[29]See Y. Itikawa, At. Data Nucl. Data Tables 14, 1 (1974) for a compendium of momentum transfer cross sections in electron collisions with atoms and molecules.
[30]Cf. H. T. Davis and L. D. Schmidt, Chem. Phys. Lett. 16, 260 (1972).
[31]A. Temkin and K. V. Vasavada, Phys. Rev. 160, 109 (1967); A. Temkin, K. V. Vasavada, E. S. Chang, and A. Silver, *ibid.* 186, 57 (1969).
[32]W. N. Sams and D. J. Kouri, J. Chem. Phys. 51, 4809 (1969); 51, 4815 (1969).
[33]A more detailed presentation of the material in Secs. II and III appears in M. A. Morrison, Ph.D. thesis (Rice University, 1976) (unpublished).
[34]Cf., S. Hara, J. Phys. Soc. Jpn. 27, 1009 (1969).
[35]P. G. Burke, N. Chandra, and F. A. Gianturco, Mol. Phys. 27, 1121 (1974); see also, N. Chandra, Phys. Rev. A 12, 2342 (1975).
[36]D. M. Chase, Phys. Rev. 104, 838 (1956); E. S. Chang and A. Temkin, Phys. Rev. Lett. 23, 399 (1969).
[37]R. W. B. Ardill and W. D. Davison, Proc. R. Soc. A 304, 465 (1968).
[38]M. E. Rose, *Elementary Theory of Angular Momentum* (Wiley, New York, 1957).
[39]M. Yoshimine and A. D. McLean, Int. J. Quantum. Chem. 1S, 313 (1967); A. D. McLean and M. Yoshimine, IBM J. Res. Dev. 12, 206 (1968); IBM J. Res. Dev. Suppl., November, 1967).
[40]E. Clementi, J. Chem. Phys. 40, 1944 (1964); IBM J. Res. Dev. Suppl. 9, 2 (1965).
[41]Cf. F. S. Acton, *Numerical Methods That (Usually) Work* (Harper and Row, New York, 1970), Chap. 4; and B. Carnahan, H. A. Luther, and J. O. Wilkes, *Applied Numerical Methods* (Wiley, New York, 1969), Chap. 2.
[42]T. E. Greville, in *Mathematical Methods for Digital Computers,* edited by A. Ralston and H. S. Wilf (Wiley, New York, 1967), Vol. II, p. 156.
[43]For example, in the static e-CO_2 potential energy, $v_\lambda^{el}(r)$ for $r = R_{O\text{-}C}$ contributes 27%, 20%, and 10% to $v_\lambda^{st}(r)$ for $\lambda = 16$, 22, and 28, respectively.
[44]M. Vucelić, Y. Öhrn, and J. R. Sabin, J. Chem. Phys. 59, 3003 (1973).
[45]A. D. Buckingham, Quantum Rev. Chem. Soc. Lond. 13, 183 (1959); see also, A. D. Buckingham, R. L. Disch, and D. A. Danner, J. Am. Chem. Soc. 90, 3104 (1968).
[46]M. E. Riley and D. G. Truhlar, J. Chem. Phys. 63, 2182 (1975); B. H. Bransden, M. R. C. McDowell, C. J. Noble, and T. Scott, J. Phys. B 9, 1301 (1967).
[47]Cf., M. A. Morrison, T. L. Estle, and N. F. Lane, *Quantum States of Atoms, Molecules, and Solids* (Prentice-Hall, Englewood Cliffs, N.J., 1976), Pt. III.
[48]S. Hara, J. Phys. Soc. Jpn. 22, 710 (1967).
[49]Applications of model exchange potentials to intermediate-energy electron-molecule collisions (10–40 eV) can be found in D. G. Truhlar and M. A. Brandt, J. Chem. Phys. 65, 3092 (1976) and D. G. Truhlar, R. E. Poling and M. A. Brandt, *ibid.* 64, 826 (1976).

[50]J. L. Franklin, Natl. Stand. Ref. Data Ser., Nat. Bur. Stand. 26, (1969).
[51]V. M. Martin, M. J. Seaton, and J. B. G. Wallace, Proc. Phys. Soc. Lond. 72, 701 (1958); L. Castillejo, J. C. Percival, and M. J. Seaton, Proc. R. Soc. Lond. A 254, 259 (1960); see also, A. Temkin and J. C. Lamkin, Phys. Rev. 121, 788 (1961); and I. H. Sloan, Proc. R. Soc. Lond. A 281, 151 (1964).
[52]N. F. Lane and R. J. W. Henry, Phys. Rev. 173, 183 (1968).
[53]J. O. Hirschfelder, C. F. Curtis, and R. B. Bird, *Molecular Theory of Gases and Liquids* (Wiley, New York, 1954), p. 950.
[54]K. Smith, *The Calculation of Atomic Collision Processes* (Wiley, New York, 1971).
[55]For a detailed presentation of the multichannel integral equations formulation, see L. A. Collins, Ph.D. thesis (Rice University, 1974) (unpublished).
[56]Cf. J. R. Taylor, *Scattering Theory* (Wiley, New York, 1972); and W. W. Bell, *Special Functions for Scientists and Engineers* (Van Nostrand, London, 1968).
[57]Cf. J. Mathews and R. L. Walker, *Mathematical Methods of Physics*, 2nd ed. (Benjamin, New York, 1970).
[58]R. A. White and E. F. Hayes, J. Chem. Phys. 57, 2985 (1972); Chem. Phys. Lett. 14, 98 (1972); J. T. Adams, R. L. Smith, and E. F. Hayes, J. Chem. Phys. 61, 2193 (1974).
[59]U. Fano, Comments At. Mol. Phys. 1, 140 (1970).
[60]To solve 32 coupled equations out to $4.0a_0$ and 5 beyond to $130a_0$ requires 1 min 42 sec of CDC 7600 time.
[61]Cf. M. Abramowitz and I. A. Stegun, *Handbook of Mathematical Functions*, Natl. Bur. Stds. (U.S. GPO, Washington, 1964), Chap. 10; J. S. Gradshtegn and I. M. Ryzhik, *Tables of Integrals, Series, and Products* (Academic, New York, 1965), p. 959.
[62]R. S. Caswell and L. C. Maximon, NBS Technical Note 409 (U.S. GPO, Washington, D. C., 1966).
[63]For example, at $k^2 = 0.005$ Ry, the converged total cross section in the SE approximation including Σ and Π symmetries is $50.9941a_0^2$, while the contribution from $m=2$ is $0.9426a_0^2$ and from $m=3$ is $0.300a_0$. See also Table II.
[64]More detailed convergence studies can be found in Chap. 8 of Ref. 33.
[65]The contributions to scattering at a given electron energy due to the various partial waves are calculated by determining the percentage of the total cross section due to each eigenphase shift. These quantities are then multiplied by the square of the components of the eigenvectors of the K matrix (in a basis of spherical harmonics). The results are summed for each partial wave, giving a quantity which reflects the relative importance of the relevant partial wave mixing in the asympotic region.
[66]D. Danner, Diplomarbeit (Universität Freiburg, 1970).
[67]N. Chandra and A. Temkin, Phys. Rev. A 13, 188 (1976).
[68]An application of such a procedure to e-H scattering is described in M. E. Riley and D. G. Truhlar, J. Chem. Phys. 65, 792 (1976).
[69]Cf. M. A. Brandt, D. G. Truhlar, and F. A. Van-Catledge, J. Chem. Phys. 64, 4957 (1976).
[70]U. Fano, Comments At. Mol. Phys. 2, 47 (1970); E. W. Chang and U. Fano, Phys. Rev. A 6, 173 (1972).
[71]G. Herzberg, *Molecular Spectra and Molecular Structure II. Infrared and Raman Spectra of Polyatomic Molecules* (Van Nostrand, New York, 1945).